Sensors & Transducers Journal, Vol. 14-1, Special Issue, March 2012, pp. 266-275

www.sensorsportal.com

Sensors & Transducers

ISSN 1726-5479

http://www.sensorsportal.com

Cell-Culture Real Time Monitoring Based on Bio-Impedance Measurements

[2] Paula DAZA, [1] Daniel CAÑETE, [1*] Alberto OLMO, [1] Juan A. GARCÍA and [1*] Alberto YÚFERA

[*] Instituto de Microelectrónica de Sevilla (IMSE), Centro Nacional de Microelectrónica (CNM-CSIC)
Universidad de Sevilla, Av. Américo Vespucio s/n. 41092. Sevilla, Spain
[1] Dto. Tecnología Electrónica, Universidad de Sevilla, Av. Reina Mercedes, s/n. 41010, Sevilla, Spain
[2] Dpt. Cell Biology, Biology Faculty, Seville University,
Av. Reina Mercedes s/n, 41012, Sevilla, Spain
E-mail: yufera@imse-cnm.csic.es, dani@zariweyo.es, aolmo@dte.us.es, hardcorejuin@gmail.com, pdaza@us.es

Received: 15 November 2011 /Accepted: 20 December 2011 /Published: 12 March 2012

Abstract: This paper proposes the application of a cell-microelectrode model in cell biometry experiments, using the cell-electrode area overlap as its main parameter. The model can be applied to cell size identification and cell count, and further extended to study cell growth and dosimetry protocols. Experiments have been conducted in AA8 cell line, obtaining promising results.

Keywords: Microelectrode, ECIS, Bio-impedance, Impedance sensor, Cell culture, Dosimetry.

1. Introduction

Many biological parameters and processes can be sensed and monitored using its impedance as marker [1-5], with the advantage of being a non-invasive and relatively cheap technique. Cell growth and activity, changes in cell composition, shape or in cell location are examples of how processes can be detected with microelectrode-cell impedance sensors [6-9]. Among Impedance Spectroscopy (IS) techniques, Electrical Cell-substrate Impedance Spectroscopy (ECIS) [7, 8], based on two-electrode setups, allows the measure of cell-culture impedances and the definition of the biological nature (material, internal activity, motility and size) of a kind of cell and its relationship with the environment

[11]. One of the drawbacks of ECIS technique is the need of efficient models to decode the electrical performance of the full system composed by the electrodes, medium and cells. Several works have been developed in this field. In [8], magnitude and phase impedance are deduced from electric field equation solution at the cell-electrode interface, giving a three parameter based model (*h*, the cell-electrode distance, R_b, cell-to-cell barrier resistance and r_{cell}, cell radius). In [9, 10], finite element simulation (FEM) is executed to solve electrical field considering the whole structure. This method gives one parameter model (R_{gap}) to describe the gap or cell-electrode region resistance. In both, the model considers cells are in confluent phase [7] or a fixed area over the electrode [9]. The latest was extended in [10] to several cell sizes, allowing to define the cell-electrode covered area as the main model parameter. In this work, an extension of the R_{gap} based model is considered, to incorporate the cell-microelectrode area overlap variable [10]. Impedance sensor sensitivity curves based on the cell size and density will be presented and applied to measure the growth rate in cell-cultures and to describe cell toxicity experiments.

In this paper, section II summarizes the electrode-solution model and complete cell-electrode characterization. The process to extract practical models is included in section III, illustrating the simulations on a simplified system leading to cell size detection. Section IV describes real time cell culture monitoring and its application to dosimetry experiments. Conclusions are highlighted in section V.

2. Electrode-electrolyte Model

The impedance of electrodes in ionic liquids has been extensively investigated. An excellent review can be found in [6]. The main components describing the electrical performance of an electrode metal inside a solution are four: the double layer capacitance, C_I, the resistance caused by the electron transfer at the electrode surface, R_{ct}, the Warburg impedance, Z_W, due to limited mass diffusion from the electrode surface to the solution, in series with R_{ct}, and the spreading resistance, R_S, the solution conductivity encountered as the current spreads out to the bulk solution. These four parameters depend on the technology, medium and geometry.

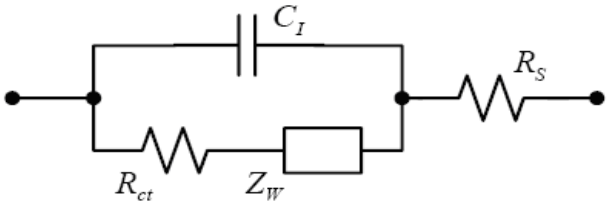

Fig. 1. Equivalent circuit for the electrode-solution interface. C_I is the double layer capacitance. Faradic impedance includes Z_w, the Warburg impedance, and R_{ct}, the charge-transfer resistance. The R_s is the spreading resistance.

3. Cell-electrode Model

Fig. 2 illustrates a two-electrode impedance sensor useful for ECIS technique: e_1 is the sensing electrode and e_2 the reference one. The e_2 electrode is commonly larger and ground connected, being its resistance small enough to be rejected. Electrodes can be manufactured in CMOS processes with metal layers [9] or using post-processing steps [13]. The cell location and size on e_1 top must be detected.

The model in Fig. 3 considers the sensing surface of e_1 can be totally or partially filled by cells. For the two-electrode sensor of Fig. 2, e_1 defines the sensing area A, and Z(ω) is the impedance by unit area of the empty electrode, without cells on top (Fig 3a). When e_1 is partially covered by cells in a surface A_c, $Z(\omega)/(A-A_c)$ is the electrode impedance associated to the uncovered area, and $Z(\omega)/A_c$ the impedance of the covered one (Fig 3b). R_{gap} models the current flowing laterally in the electrode-cell interface, which depends on the electrode-cell distance at the interface (in the range of 15-150 nm). The R_s is the spreading resistance through the conductive solution. For an empty electrode, the impedance model $Z(\omega)$ is represented by the circuit in Fig. 2. It has been considered for e_2 the model in Fig 3a, not covered by cells. The e_2 electrode is commonly larger and ground connected, being its resistance small enough to be rejected.

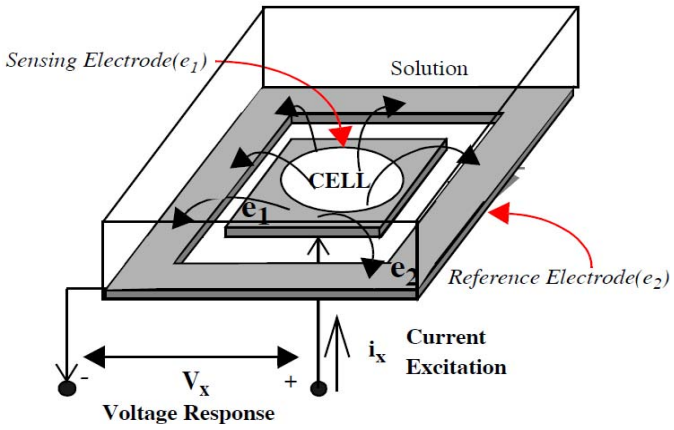

Fig. 2. Two electrodes for ECIS: e_1 (sensing) and e_2 (reference). AC current i_x is injected between e_1-e_2, and voltage response V_x is measured.

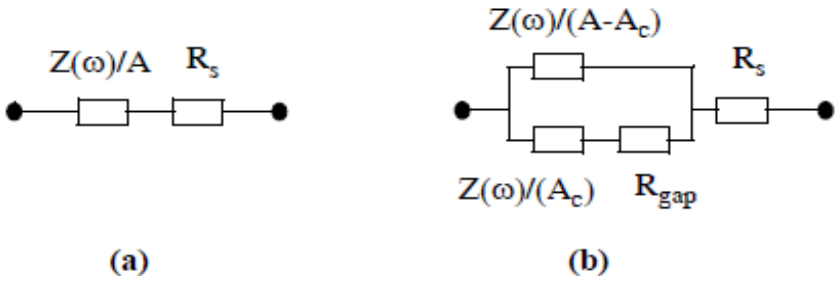

Fig. 3. Proposed model for the electrode-solution-cell system with area *A*, uncovered with cells (a), and covered with area A_c (b).

Fig. 4 represents the impedance magnitude, Z_c, for the sensor system in Fig. 2, considering that e_1 could be either empty, partially or totally covered by cells. The parameter *ff*, fill factor, can be zero for $A_c=0$ (e_1 electrode empty), and 1 for $A_c=A$ (e_1 electrode full). It is defined Z_c *(ff = 0)* = Z_{nc} as the impedance magnitude of the sensor without cells.

The relative change of the impedance magnitude is defined as

$$r = \frac{Z_c - Z_{nc}}{Z_{nc}}, \tag{1}$$

which informs more accurately from these variations, being *r* the change of impedance magnitude for the two-electrode with cells (Z_c) with respect to the system without them (Z_{nc}). The graphics of *r*

versus frequency are plotted in Fig. 5, for a cell-electrode coverage ff from 0.1 to 0.9 in steps of 0.1, using an R_{gap} = 90 kΩ. The size of the electrode is 32 × 32 μm^2, as in [9, 10]. The frequency where the sensitivity to cells is higher can be identified at 100 kHz, represented by *r* increments, in accordance with previous results [9, 10]. For a given frequency, each normalized impedance value of *r* can be linked with its *ff*, being possible the cell detection and the estimation of the covered area A_c. Even more, the area covered can be interpreted as a specific number of cells, allowing cell count for a given cell size.

From Fig. 5, it can be deduced that models of electrode-cell electrical performance can be used to derive the overlapping area in cell-electrode systems, useful for biological studies. It can be observed how the curve fits well with the frequency range, placing the maximum *r* value around 100 kHz, as predicted by FEM simulations [9, 10]. A value of R_{gap} = 90 kΩ was selected for this curve, representing a maximum value of the r curve with *ff* = 0.69, which represents the ratio (A_c/*A*), for a cell size of 30 μm diameter showed at figure obtained using FEM simulations [10]. Impedance sensor curves at Figs. 4 and 5 were obtained using SpectreHDL [15] mixed-mode simulator, with Analog Hardware Description Language (AHDL) for circuits in Fig. 3. An advantage of using AHDL models is the possibility of including non-linear performance of circuit elements, in our case, the frequency squared-root function at the Warburg impedance.

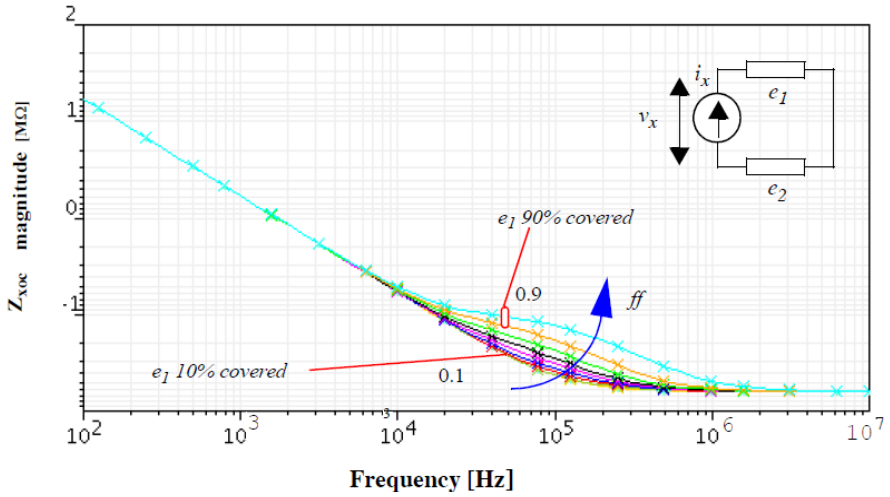

Fig. 4. Impedance evolution when fill factor increases (electrode size of 32 × 32 μm^2).

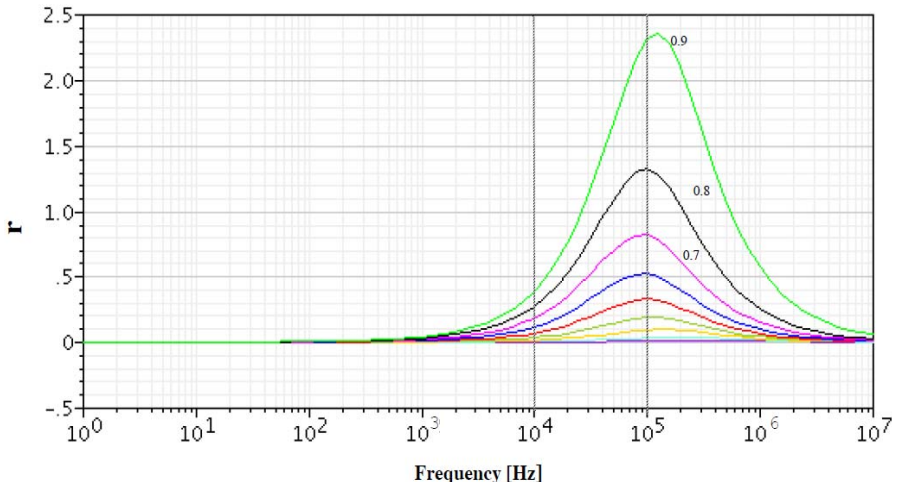

Fig. 5. Normalized impedance *r* versus frequency derived from Fig. 4. Curves correspond to *ff* in the range of 0.1 (near empty) to 0.9 (near full).

4. Cell Culture Applications

4.1. Electrode Model

The proposed model in Fig. 3 has three main parameters: the electrode area (*A*), fill-factor (*ff*), and the resistance of the gap region (R_{gap}). Technology data were included and simulation results obtained to model a commercial electrode: 8W10E, from Applied Biophysics [12]. It is composed by eight wells, each one containing ten circular gold microelectrodes of 250 μm diameter. Ten sensing electrodes, in parallel, were used for e_1 and only one common reference electrode is used, much larger than the sensing ones.

Fig. 6 represents the normalized impedance r expected for these electrodes. For R_{gap} = 22 kΩ, the fill factor changes from electrodes without cells on top (*ff* = 0.1) to those fully covered (*ff* = 0.9). Values of R_{gap} can be used to match the models to observed performance. In Fig. 7, R_{gap} values were changed for *ff* = 0.9, observing large changes in *r*. Finally, the electrode area was also modified for R_{gap} = 22 kΩ and *ff* = 0.9, showing the results in Fig. 8. It can be observed that the optimal working frequency is close to the one proposed by the electrode manufacturer (around 4 kHz), and that electrode area covered by cells can be approximated by using the fill factor parameters. The performance curves obtained before can be used to fit experimental results to the proposed model and find relevant biometric characteristics.

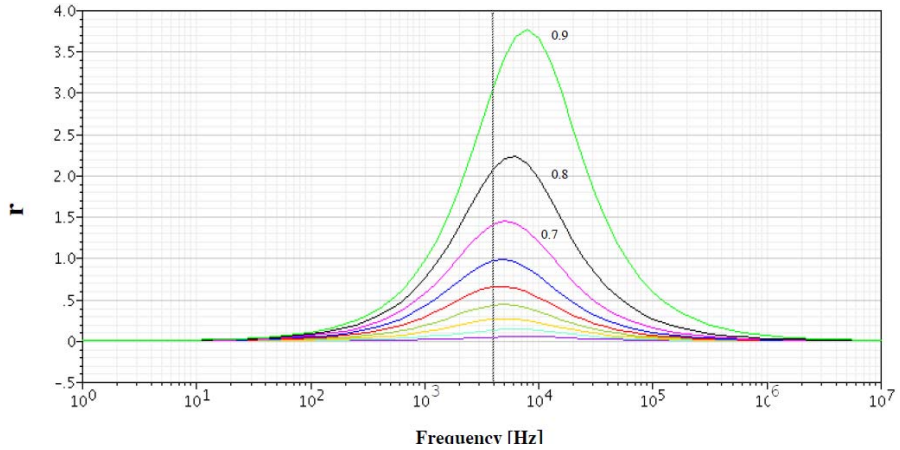

Fig. 6. Curves obtained for *r* vs frequency, for *ff* ∈ [0.1, 0.9] and R_{gap} = 22 kΩ, using 8W10E electrodes.

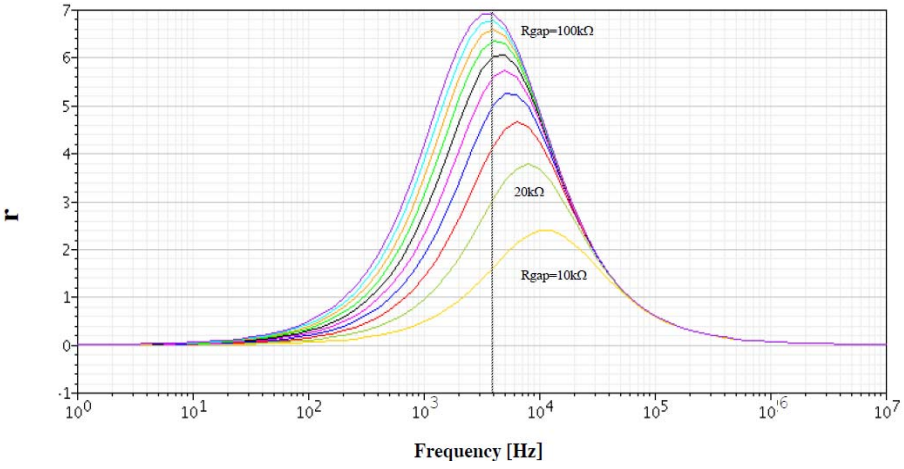

Fig. 7. Curves obtained for *r* vs frequency, for R_{gap} ∈ [10 kΩ, 100 kΩ] in steps of 10 kΩ, for *ff* = 0.9, using 8W10E electrodes.

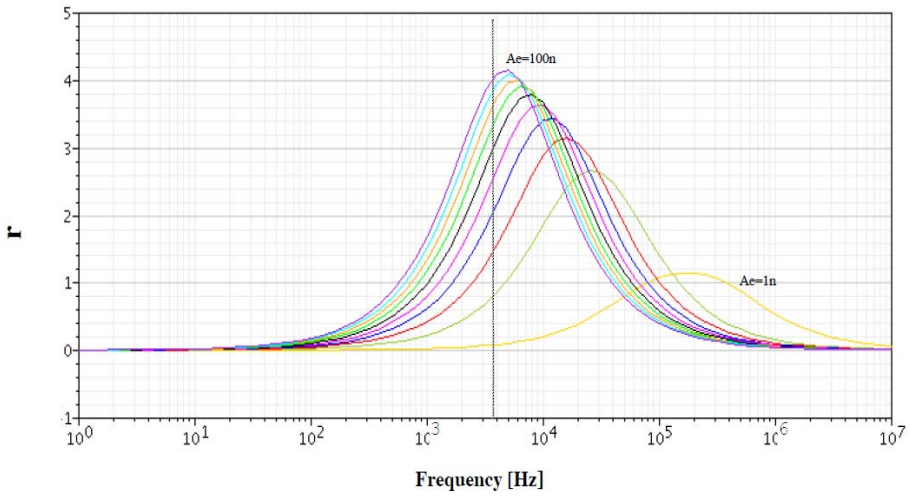

Fig. 8. Curves obtained for *r* vs frequency, for R_{gap}= 22 kΩ and *ff* = 0.9, for different electrode areas (1 n to 100 n). 49 n ($49.10^{-9}m^2$ corresponds to a circular electrode with a 250 μm diameter).

4.2. Cell Growth

Cell growth experiments in AA8 cell line have been conducted using 8W10E sensors. A similar setup to [8] was used. AA8 cells from Chinese hamster were seeded initially, in an approximated number of 5000, and growth was monitored during seven days. In Fig. 9a the impedance evolution of the experiment is shown. The impedance range is around 1220 Ω (380 Ω - 1600 Ω). Considering the initial cell number of 5000 as very low, we can take the initial impedance as the no-cell impedance value (Z_{nc}). At t = 6000 min, the medium was changed, and the confluent phase was achieved at approximately t = 8500 min. The maximum experimental value given from eq. (1) is around *r* = 3.1, as illustrates Fig. 9b. We consider in our model that the electrodes are approximately fully covered by cells for *ff* = 0.9. The value of R_{gap} that better fits is 22 kΩ. System response corresponds to *r*-values illustrated in Fig. 6. From these curves, it can be obtained the fill factor at different times. Table 1 summarizes the relative normalized impedance values *r* at several times. Using Fig. 6 for the sensor response, the fill factor is calculated at every instant. For a well area of 0.8 cm^2, the maximum cell number goes from 0.8×10^6 to $1.6x10^6$. Number of cells, n_{cell}, in Table 1, is obtained from 0.8×10^6 expected final cell number. A value of Z_{nc} = 380 Ω for *r* calculus in eq. (1) was considered.

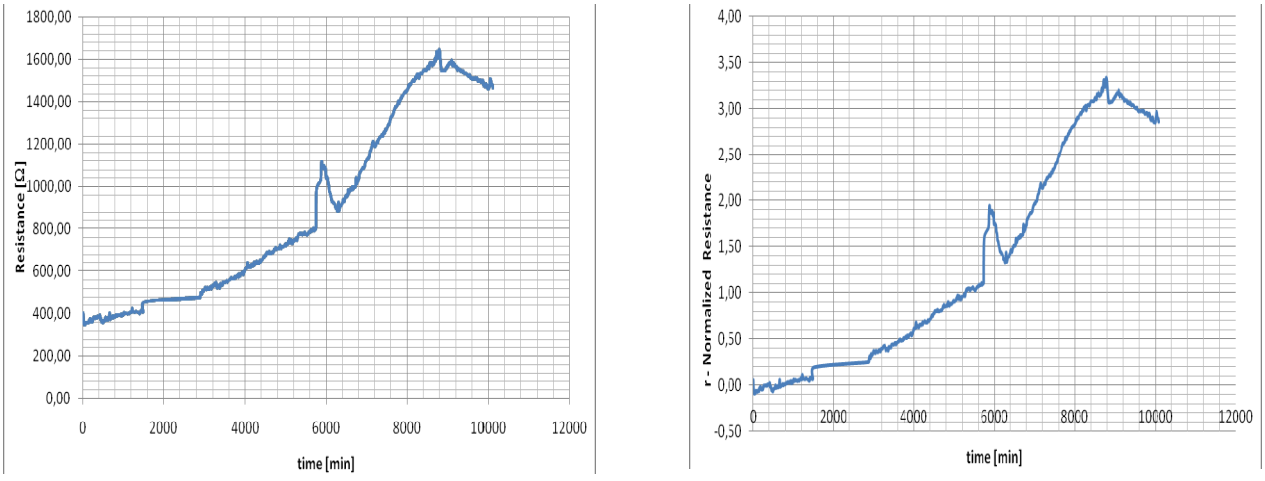

(a) (b)

Fig. 9. (a) Impedance evolution of the cell growth experiment; (b) Normalized impedance *r* evolution obtained.

Table 1. Cell number (n_{cell}) obtained from impedance Z_c measure in Fig. 9, using the *r* curves proposed for 8W10E sensors.

t (min)	r	ff	n_{cell}
0	0	-	5000
500	0.024	0.020	18000
1000	0.050	0.050	44000
1500	0.072	0.070	63000
2000	n.a.	n.a.	n.a.
2500	n.a.	n.a.	n.a.
3000	0.374	0.362	322000
3500	0.437	0.395	351000
4000	0.615	0.475	422000
4500	0.777	0.530	471000
5000	0.903	0.581	516000
5500	1.033	0.602	535000
6000	1.074	0.620	551000
6500	1.507	0.710	631000
7000	1,970	0.775	689000
7500	2,353	0.810	720000
8000	2,837	0.860	764000
8500	3.113	0.890	791000
9000	3.134	0.900	800000
9500	3.010	0.875	778000
10000	2,857	0.864	768000

4.3. Dosimetry

Experiments to characterize the influence of several drugs in cell growth were performed. The objective was to prove that the proposed model allows counting the cell number at different doses. It was considered the AA8 cell line and six different doses of MG132 for growth inhibition (from 0.2 μM to 50 μM). 8W10E sensors were also used to carry out the dosimetry experiments.

After 72 hours of normal cell growth, the medium was changed and the drug added at different doses: 0.2, 0.5, 1, 5, 10 and 50 μM for wells 3 to 8 respectively. Well 2 was the control. Measured impedances for the 8 wells are shown in Fig. 10, for 4 kHz working frequency. At the end of the experiment it can be observed that the impedance decreases as the drug doses increases. Control (W2) is full of cells with the maximum impedance, while the maximum dose (W8) has the lowest resistance, at the bottom. The black line (W1) represents the electrode-solution impedance. After the medium changes (t = 4000 min), it is observed a decreasing impedance below the initial baseline level (400 Ω) that we cannot explain. Final impedance values at 8000 min, Z_c, were considered, at Table 2. From Z_{nc} and Z_c, *r* values are calculated in the third column. Using curves for r versus frequency in Fig. 6, the *ff* estimated values from proposed model are obtained. The cell number at the end of the experiment was also counted and shown at the last column for each well. Considering ff_{max} = 0.9 for a measured cell number of 8.06×10^5, the expected values for *ff* are calculated.

The same data are summarized in Table 3 for 2, 4 and 10 kHz frequencies respectively. The better agreement is obtained at 4 kHz in fill factor (*ff*). It is observed that the impedance baseline, Z_{nc}, for *r* calculus decreases with frequency probably due to electrode impedance dependence. For medium resistance (W1) and high drug concentrations wells (W6-W8), the resistance measured is below Z_{nc}, so eq. (1) cannot be applied for *r* calculation.

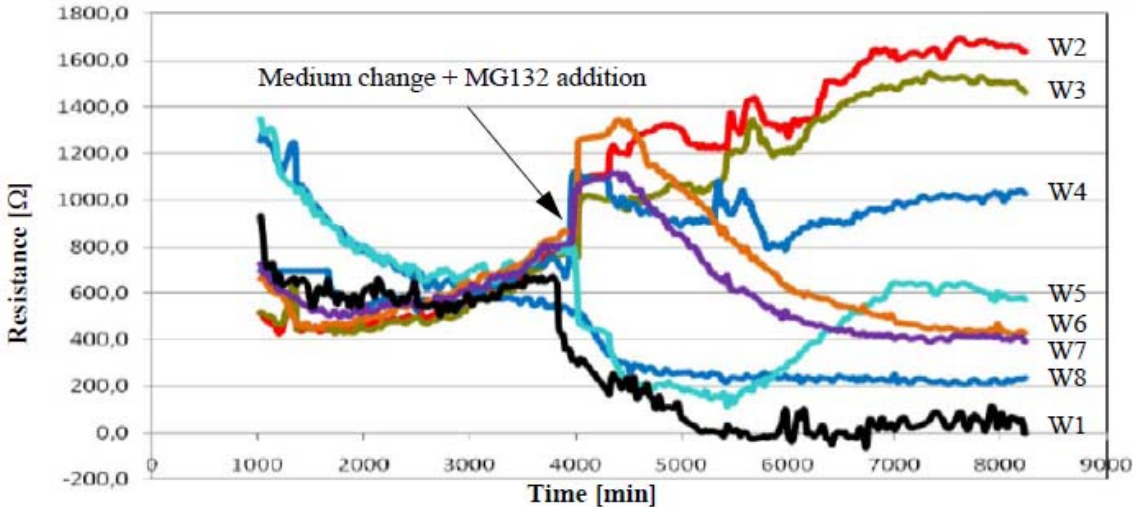

Fig. 10. Impedance measure in dosimetry at 8 wells for 4 kHz frequency. W1: Medium. W2: Control. W3: 0.2 μM. W4: 0.5 μM. W5: 1 μM. W6: 5 μM. W7: 10 μM and W8: 50 μM.

Table 2. Experimental values for relative impedance (r) and fill-factor (ff) for Z_{nc} = 400 Ω at a frequency of 4 kHz.

Well	Z_c t=8000min	r Z_c ,Z_{nc}	ff estimated	ff expected	n_{cell} measured
1	259.2	-	-	-	Medium
2	1631.7	3.1	0.90	0.900	8.06×10^5
3	1454.7	2.6	0.85	0.690	6.13×10^5
4	1030.6	1.5	0.72	0.610	5.41×10^5
5	625.8	0.5	0.44	0.410	3.60×10^5
6	417.4	0.05	0.037	0.036	3.20×10^4
7	406.8	0.015	0.016	0.024	2.10×10^4
8	99.6	< 0	-	0.005	4.00×10^3

Table 3. Experimental values for relative impedance (r) and fill-factor (ff) for Z_{nc} = 480 Ω, 400 Ω and 315 Ω, at 2, 4 and 10 kHz working frequencies respectively.

	r (from Z_c and Z_{nc})			ff (from model)			
Well	2 kHz	4 kHz	10 kHz	2 kHz	4 kHz	10 kHz	ff expect.
1	-	-	-	-	-	-	Medium
2	2.43	3.1	3.76	0.98	0.90	0.90	0.900
3	2.18	2.6	3.24	0.94	0.85	0.88	0.690
4	1.17	1.5	2.21	0.82	0.72	0.82	0.610
5	0.21	0.5	0.84	0.32	0.44	0.44	0.410
6	-	0.05	-	-	0.037	-	0.036
7	-	0.015	-	-	0.016	-	0.024
8	-	-	-	-	-	-	0.005

5. Conclusions

This work describes an area-dependent model for cell-electrode systems and its application to measure and identify cells during cell culture protocols. A practical circuit for electrode-solution-cell simulation was employed, using an AHDL description for commercial electrodes, obtaining a good matching. Optimal measurement frequency was identified near 4 kHz. A cell growth evolution study based on 8W10E electrode models is presented. Curves obtained experimentally allow the real time growth monitoring by fitting the R_{gap} parameter. An estimation of the number of cells was obtained by using sensor curves calculated from the electrical model proposed. Dosimetry experiments reproduce similar conditions to cell growth, but in this case, a growth inhibitor is added at different doses. A decreasing impedance is observed, below the baseline expected (Z_{nc}) that we cannot explain. However, for the control and small drug doses, impedance curves are perfectly aligned. A proposed model with R_{gap} = 22 kΩ was fitted to explain experimental data. Deviations from data are over 10-20 % in fill factor, more accurate for 4 kHz.

The deviations in fill factors measured are not small, being required to analyze the influence of error sources to increase the system performance. First, Signal-to-Noise Ratio (SNR) should be increased at the setup. Second, the proposed model has the advantage that it only needs one parameter (R_{gap}), versus other reported models using three parameters [8]. One parameter model makes it easy to fit the experimental data, but it can introduce inaccuracy. The possibility to add more parameters to the model should be considered in the future.

Acknowledgements

Part of this work was carried out thanks the financial help from the project: “Auto-calibración y auto-test en circuitos analógicos, mixtos y de radio frecuencia: Andalusian Government project P0-TIC-5386”, co-financed with FEDER program. We also want to thank Citoquimica Ultraestructural Group (BIO132) of Cell Biology Department, Biology Faculty, Seville University, for its valuable help in the lab to develop the cell culture experiments.

References

[1]. S. Grimnes and O. Martinsen, Bio-impedance and Bioelectricity Basics, 2nd edition, *Academic Press, Elsevier*, 2008.
[2]. R. D. Beach et al., Towards a Miniature In Vivo Telemetry Monitoring System Dynamically Configurable as a Potentiostat or Galvanostat for Two- and Three- Electrode Biosensors, *IEEE Transaction on Instrumentation and Measurement*, Vol. 54, No. 1, 2005, pp. 61-72.
[3]. A. Yúfera et al., A Tissue Impedance Measurement Chip for Myocardial Ischemia Detection, *IEEE Transaction on Circuits and Systems: Part I*., Vol. 52, No. 12, 2005, pp. 2620-2628.
[4]. S. Radke et al., Design and Fabrication of a Microimpedance Biosensor for Bacterial Detection, *IEEE Sensor Journal*, Vol. 4, No. 4, 2004, pp. 434-440.
[5]. A. Yúfera and A. Rueda, A Method for Bioimpedance Measure with Four- and Two-Electrode Sensor Systems, in *Proceedings of the 30th Annual International IEEE EMBS Conference*, 2008, pp. 2318-2321.
[6]. D. A. Borkholder. Cell-Based Biosensors Using Microelectrodes, PhD Thesis, *Stanford University*, 1998.
[7]. I. Giaever, et al., Use of Electric Fields to Monitor the Dynamical Aspect of Cell Behaviour in Tissue Cultures, *IEEE Transaction on Biomedical Engineering*, BME-33, No. 2, 1986, pp. 242-247.
[8]. I. Giaever and C. R. Keese, Micromotion of mammalian cells measured electrically, *Proc. Nail. Acad. Sci. USA. Cell Biology*, Vol. 88, Sep. 1991, pp. 7896-7900.
[9]. X. Huang et al., Simulation of Microelectrode Impedance Changes Due to Cell Growth, *IEEE Sensors Journal*, Vol. 4, No. 5, 2004, pp. 576-583.

[10].A. Olmo and A. Yúfera, Computer Simulation of Microelectrode Based Bio-Impedance Measurements With COMSOL, *BIODEVICES 2010,* Valencia (Spain), 20-23, Jan. 2010, pp. 178-182.
[11].P. Wang and Q. Liu, editors, Cell-Based Biosensors: Principles and Applications, *Artech House Series*, 2010.
[12].Applied Biophysics, http://www.biophysics.com/
[13].A. Manickam, A. Chevalier, M. McDermott, A. D. Ellington, and A. Hassibi, A CMOS Electrochemical Impedance Spectroscopy (EIS) Biosensor Array, *IEEE Transactions on Biomedical Circuits and Systems*, BME-4, No. 6, 2010, pp. 379-390.
[14].A. Yúfera and A. Rueda, Design of a CMOS closed-loop system with applications to bio-impedance measurements, *Microelectronics Journal*, Vol. 41, 2010, pp. 231-239.
[15].A. Yúfera A. and E. Gallego, Generation of HDL Models for Bioimpedance Sensor Simulation Based on Microelectrodes, *Sensors and Transducers*, Vol. 10, Special Issue, February 2011, pp. 160-170.
